MULTI-MODAL ACOUSTIC POWER CHARACTERISATION OF DUCTED ELEMENTS

Yackine TADJOU[1,2], Jean-Daniel CHAZOT[2],
Emmanuel PERREY-DEBAIN[2], Arnaud PLESSY[1]

[1] *CRITT M2A, Parc de la Porte Nord, Rue Christophe Colomb, 62700 Bruay-la-Buissière, France*

[2] *Laboratoire Roberval, Université de Technologie de Compiègne, 60205 Compiègne BP20529, France*

SUMMARY

Passenger vehicle outside and inside noise is more and more of concern with harder regulations but also new emerging powertrains like electric, hybrid or hydrogen. In this context, in-duct noise concerns several components, and a focus is made on forced induction systems like compressors or turbochargers. To achieve a multimodal and non-intrusive measurement, an optimization of sensors position is realized with a genetic algorithm noticeably. The effect of measurement uncertainty, turbulence and its denoising is also studied.

INTRODUCTION

Current automotive NVH challenges are primary the noise reduction for homologation tests but also for passenger comfort. A good knowledge of each component is primordial to reduce prototyping and test costs. Following harder regulations in CO_2 emissions, downsizing of powertrains made forced induction systems to develop more and more on light passenger vehicles. Nowadays, more than a half of cars in circulation have a turbocharger (TC)[1], and its noise contributes to the overall noise. In this industrial context, the CRITT M2A, an independent research & development and test center for automotive industry has the opportunity to work on advanced in-duct noise characterization of turbochargers. The objective is to develop a measurement method of turbocharger active and passive noise on the full human audible range over its whole operating points.

The turbocharger is a radial rotating machine composed of a shaft with two wheels, one for the compressor part and one for the turbine. Both stages have an inlet duct and an outlet one. Here only the compressor stage is studied. The turbocharger generates a broadband noise that propagates in both ducts with tonal components linked to the rotational speed. This noise is under a flow which is uniform while not considering close field (~2 diameters), can reach 250 °C for small turbochargers, a Mach number M_a of 0.3 and a relative static pressure of 1 bar. Measuring acoustic pressure in this

environment is challenging also in terms of compactness but work have already been published on this subject.

The Royal Institute of Technology in Stockholm (KTH) have been working on this subject for approximately 20 years and started with plane wave characterization. They used the 2-port method to get the passive and active turbocharger characteristics on some operating points [2]. They also worked on denoising method based on spacing the microphone far apart to get rid of the spatial correlation of the noise generated in the turbulent boundary layer of the flow. An extension of this work in the multi-modal domain with the 2N-port method can be found in [3]. Several optimisation techniques of the modal decompositions have been presented, like constrained microphone positioning [4], the use of genetic algorithm [3] or Artificial Neural Networks with the help of CFD data [5].

The full compressor map have been studied by I. James for the plane wave only using a beamforming method with the CRITT M2A [6]. Passive measurements have been carried out to get the scattering matrix of the turbocharger in static and active conditions. Operating noise have been measured on a full map with an automated and synchronized measurement between turbocharger test bench and acoustic acquisition. The use of anechoic termination helped to get an active noise independent of the test bench. All measurements have been compared to the one obtained on engine test-bench, on vehicle and simulations for validation with good agreement.

The propagation of acoustic waves in ducts in a multimodal context has been well studied by the Roberval Laboratory of the University of Technology of Compiègne with several research projects on cylindrical and rectangular ducts. Multimodal acoustics characterisations of air conditioning systems [7] or passive elements [8] have been done on rectangular ducts using the 2N-port method with a dedicated bench with a limited flow speed.

The presented work here are the basics of the development of a measurement method. Using the experience of cited references, the goal is to characterize all the operating points of the TC, in a multimodal context using the 2N-port method in cylindrical ducts. For an efficient use of the 2N-port method, the modal decomposition must be accurate and denoising techniques have to be used. The last two points are discussed in the present work.

IN-DUCT ACOUSTICS

In-duct acoustic pressure propagation can be separated in two domains, the plane wave one and the multi-modal one. For the former, acoustic pressure is constant over a cross-section of the duct and for the latter it is dependent of the transversal directions. Using an $e^{-i\omega t}$ convention, in a cylindrical duct, it can be decomposed as a sum of propagating modes with *m,n* indices for azimuthal and radial orders each one with a corresponding amplitude $A_{mn}^{\pm}$:

$$p(r,\theta,z) = \sum_{m=-\infty}^{+\infty} \sum_{n=0}^{+\infty} N_{mn} J_m\left(\frac{\chi_{mn} r}{a}\right) e^{im\theta}\left(A_{mn}^{+} e^{ik_{z,mn}^{+} z} + A_{mn}^{-} e^{ik_{z,mn}^{-} z}\right) \quad (1)$$

The acoustic pressure measured at the inner wall of a cylinder of radius of a is presented in equation (1) and takes in account a flow with uniform velocity inside axial modal wavenumbers $k_{z,mn}^{\pm}$ described in equation (2) in which k is the wavenumber. J_m are the first kind Bessel function of m order and χ_{mn} zeros of its derivatives. Each mode amplitude $A_{mn}^{\pm}$ is normalized with N_{mn} using mode orthogonality property. Plus and minus symbols respectively show positive z propagation and negative z propagation, flow being considered in positive direction and

$$k_{z,mn}^{\pm} = \frac{-M_a k \pm \sqrt{k^2 - (1 - M_a^2)\frac{\chi_{mn}^2}{a}}}{1 - M_a^2}. \quad (2)$$

Each mode has a frequency cut-off dependent on the sound velocity c_0 from which it is propagative and evanescent below this frequency. The equation (3) is obtained for each modal wavenumber when the square root in equation (2) is zero:

$$f_{c,mn} = \frac{\chi_{mn} c_0 \sqrt{1 - M_a^2}}{2\pi a} \tag{3}$$

The equation (1) can be first put in matrix form with the pressure being the product between the collocation matrix $\boldsymbol{\phi}$ of the $2N$ modal functions in r, θ and z upstream and downstream evaluated at the M microphones and the vector of modal amplitudes:

$$\boldsymbol{p} = \boldsymbol{\phi A} \tag{4}$$

With $\phi_{i,mn}^{\pm}$ being written at the ith microphone and mn mode order:

$$\phi_{i,mn}^{\pm} = N_{mn} J_m \left(\frac{\chi_{mn} r_i}{a}\right) e^{-im\theta_i} e^{ik_{z,mn}^{\pm} z_i} \tag{5}$$

In the context of uncoherent phenomena like flow with turbulences, the use of quadratic quantities allows denoising techniques as explained further in this paper. Equation (6) is obtained by multiplying equation (4) by its conjugated transpose noted ^{H} with $\boldsymbol{S}_{pp}$ being the measured interspectral matrix, with autospectra on its diagonal and interspectra off-diagonal and $\boldsymbol{S}_{AA}$ the intermodal matrix with modal amplitudes on its diagonal and modal coherence off-diagonal.

$$\boldsymbol{S}_{pp} = \boldsymbol{\phi S}_{AA} \boldsymbol{\phi}^H \tag{6}$$

For an intrinsic measure of the acoustic properties of a component, the acoustic power is a great indicator. It can be obtained from the acoustic intensity which comes from acoustic pressure and velocity as described by Morphey [9]. Multimodal acoustic power under uniform flow with a ρ_0 density in a cylindrical duct for both directions W_{mn} can then be written from modal amplitudes:

$$W_{mn}^{\pm} = \frac{|A_{mn}^{\pm}|^2}{2\rho_0 c_0} \left(M_a - \frac{k_{z,mn}^{\pm} (1 + M_a)^2}{M_a k_{z,mn}^{\pm} - k} \right) \tag{7}$$

The total power is recovered as:

$$W_{tot}^{\pm} = \sum_{m=-\infty}^{+\infty} \sum_{n=0}^{+\infty} W_{mn}^{\pm} \tag{8}$$

MODAL DECOMPOSITION OPTIMISATION

To get the modal amplitudes, the collocation matrix $\boldsymbol{\phi}$ must be inverted whatever the formulation used. Therefore, a Moore-Penrose pseudo-inverse symbolized by † of itself is required giving the following equation in quadratic formulation:

$$\boldsymbol{S}_{\hat{A}\hat{A}} = \boldsymbol{\phi}^{\dagger} \boldsymbol{S}_{\hat{p}\hat{p}} \boldsymbol{\phi}^{H^{\dagger}} \tag{9}$$

Here, the hat symbol refers to measured quantities. This way of inversion gives the best solution of $\boldsymbol{S}_{\hat{A}\hat{A}}$ talking about least mean squares. The condition number of the matrix $\boldsymbol{\phi}$ is an indicator that shows the stability to small perturbations when the matrix is inverted. This operation is done at each frequency of the problem. Considering an accurate model for mode decomposition, the condition number could be optimized by varying microphone positions. So, two approaches of positioning are taken resulting in several arrays that are compared using the condition number. One can note that to keep a non-intrusive setup, microphones can only be flush mounted to the cylinder wall. It is shown later on Figure 3 that for a basic microphone positioning, radial modes are difficult to distinguish. This is because each have the same pattern along the circumference as well as the plane wave mode.

Deterministic arrays

Separation of modes can be approached independently for radial, azimuthal and axial directions. Incident and reflected modes can also be decomposed independently. Åbom and Bodèn showed in [10] that the use of at least 3 axial microphones can allow both close and far spacing to maximize the valid frequency band. Having $M \geq 3$ in z direction also overdetermines the problem for upstream and downstream waves separation. The decomposition of azimuthal modes can also be treated with the Shannon criteria. Tapken and Enghardt show in [11] that there should be at least $2m$ microphones spaced on θ over a single section. For radial modes, each ϕ_i terms of equation (5(5) are close to equal resulting in an singular ϕ matrix and an imprecise modal amplitude estimation. To avoid this situation it is possible to maximize the axial space between the farthest microphones. This emphasis phase difference ($k_{z,mn}\, z_i$) between each radial mode and the plane wave one for a better decomposition. Solving these constraints ends in a ring pattern on several non-uniformly spaced sections as shown in [4]. Another way of positioning the microphones is to follow an helix pattern as shown later.

Random and genetic algorithm arrays

A random array is created with a constraint of non-coincidence taking in account a ¼ inches microphone with an additional dead-space. Developing the idea of random positioning a genetic algorithm is used to test more random positions as well as in the work of Sack, Åbom and Efraimsson in [3]. A genetic algorithm (GA) is a process which minimizes a cost function based on the natural selection principle. Here, the cost function is the sum of the condition number for each frequency with frequency mode cut-offs excluded. One individual is one arrangement with $2M$ random generated variables because only z_i and θ_i coordinates can be modified. The population is the number of individuals generated at each generation. At each generation, some of the best individuals are selected and directly sent to the next generation. A fraction of the population is crossed, which means solutions of coordinates are mixed to create new individuals. The last individuals are mutated, so their coordinates are slightly modified still with the non-coincidence constraint. With passing generations, the cost function decreases until a stop criterion is reached. In this study the stop criterion chosen is a ceil of variation from a generation to another to make sure all behaviours can be seen, and the algorithm setup improved for better and faster results. With this criterion, a parametric study shown in Figure 1 is conducted to determine the maximum measurement length z_{max}, and the microphone number with 10 as the maximum condition number allowed.

Figure 1 : Parametric studies:

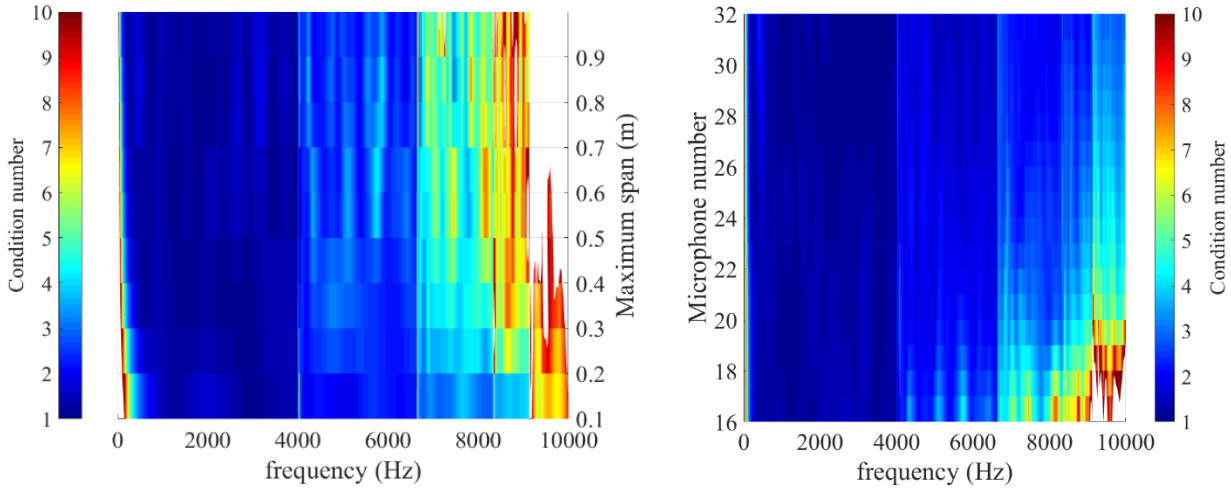

Left (Fixed Microphone number: M=16), Right (Fixed Span : z_{max} = 0.55m)

A pitch of 0.1 mm is set for the mesh to ensure the solution can be done by machining under standard tolerances for the future experimental work. The left part of the Figure 1 shows that a

maximum measurement length of 0.325 m is a good compromise between high and low frequencies accuracy. The right part of the Figure 1 shows an acceptable minimum of 20 microphones.

Comparison

The condition number $\kappa(\phi)$ in function of the frequency is computed for four different microphone arrays as described above. At each frequency cut-off in equation (3), a peak of conditioning appears due to the modal decomposition model. At these specific frequencies, the axial wavenumber is small and separation of upstream and downstream waves is nearly impossible. This results in a singular matrix.

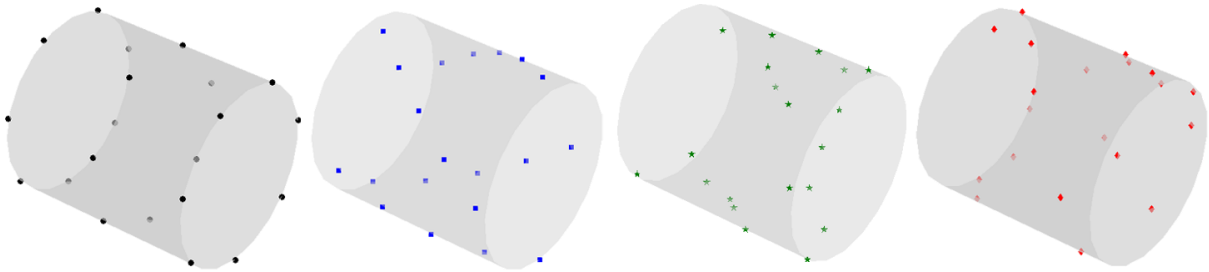

*Figure 2: Representation of microphone arrays: Black (**Ring**), Blue (**Helix**), Green (**Random**), Red (**GA**)*

Random or Genetic Algorithm approaches generally show better results than Deterministic ones. Parametric studies for each array showed that deterministic ones need a higher number of microphones for better results. The span of the array also has a great impact on deterministic positioning making them bigger for the same performances and then not convenient for experimental setups. Taking in account all these constraints, an array of 20 microphones over a total duct length of 0.325 m and a 0.025 m radius is chosen.

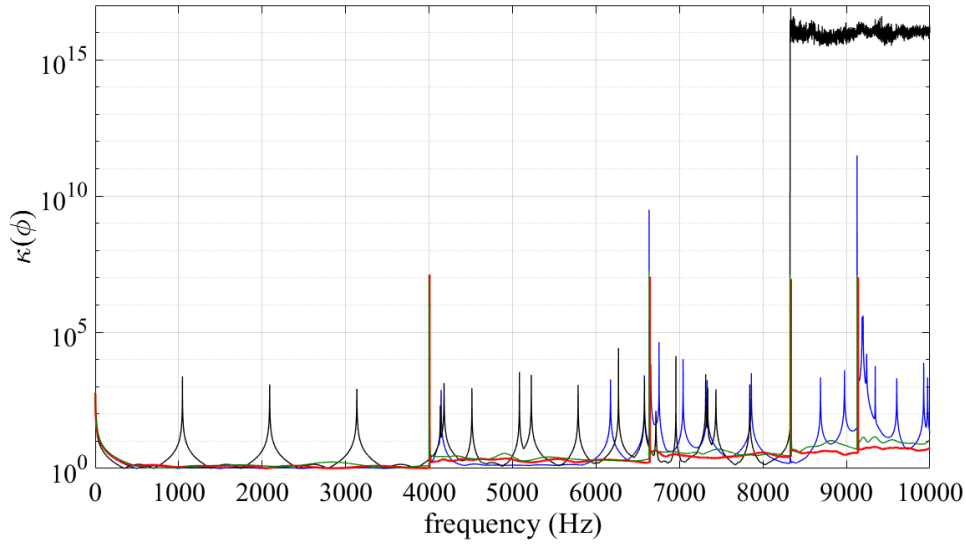

*Figure 3 : Condition number in function of frequency for each configuration: Black (**Ring**), Blue (**Helix**), Green (**Random**), Red (**GA**)*

As shown in [4], deterministic arrays can easily show “weak singularities” in the condition number due to coupling between modes of same m order, but also different order and shapes. The situation can occur because of the existence of a correlation between the regular microphone spacing and the regular mode shapes. Some of these singularities are periodic and unavoidable. Therefore “random” arrays give good results because they overcome constraints with irregular spacing in all directions.

The Figure 3 shows that the condition number of the ring array has periodic singularities around 10^4 for the whole spectrum and very high ones at 10^{15} from the first radial mode (0,1) to the maximum frequency of the study. This makes modal decomposition impossible above 8290 Hz with this array. The helix array also shows periodic singularities but can decompose modes on the whole

frequency range. The random array doesn't show singularities except at frequency cut-off of modes and has a condition number in the order of 10^1. The Genetic Algorithm array shows even better results way below 10 from 60 Hz to 10 kHz.

UNCERTAINTIES MODELISATION

A parametric study is conducted to evaluate the impact of uncertainties due to the measurement chain, the noise generated in the turbulent boundary layer (TBL) on the multi-modal acoustic power computed from pressure measurement and the performances of a denoising technique. To do so, a theoretical intermodal matrix $\boldsymbol{S}_{AA}$ is synthesized with unitary amplitudes for the chosen propagative modes on the diagonal and intermodal coherence terms $\gamma_{mn,m'n'}$ off-diagonal. Synthesized acoustic pressure is then obtained with equation (6) using the GA optimized matrix. The perturbation is then added in order to create a noised interspectral pressure matrix $\boldsymbol{S}_{\hat{p}\hat{p}}$ (in the case of an experiment this $\boldsymbol{S}_{\hat{p}\hat{p}}$ matrix would be the measured matrix). The case of a TBL noise is also considered using a Corcos model.

Measurement chain uncertainty

The measurement chain is composed of a 1/4inches piezo resistive pressure sensor Kistler 601CAA, an in-line charge converter PCB 422E51 a PAK MKII analyser a computer. Only the sensor and the in-line converter have a significant uncertainty value of respectively 0.03 % and 1 %. These uncertainties are summed and rounded to the next unity to overestimate it at $n = 2$ %. The noised interspectral matrix $\boldsymbol{S}_{\hat{p}\hat{p}}$ is defined as:

$$\boldsymbol{S}_{\hat{p}\hat{p}} = \boldsymbol{S}_{pp}(1+n) \tag{10}$$

The theoretical and noised acoustic power is then computed for each mode and shown in Figure 4. It is clear that this level of uncertainty has little influence on the resulting acoustic power with a maximum of 1 dB of uncertainty. These results also validate microphones position optimization using GA.

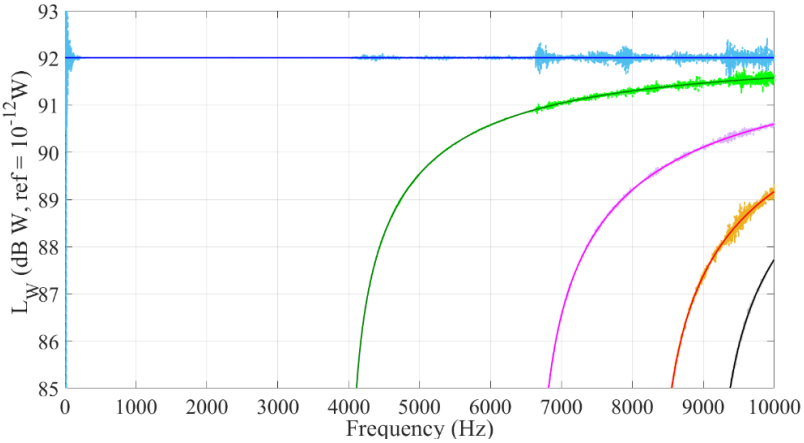

Figure 4 : Acoustic power of in-duct propagating modes:
Blue : mode (0,0), Green : mode (1,0), Magenta : mode (2,0), Red : mode (0,1), Cyan : mode (3,0) ;
Thick line : Theoretical, Light line : Noised

Turbulent boundary layer noise

The noised signal can be modeled as the sum of the unnoised signal $\boldsymbol{S}_{pp}$ and the TBL noise $\hat{\boldsymbol{\Gamma}}$ which is the term to term product between the complex coherence matrix $\boldsymbol{\Gamma}$ and a diagonal matrix $\boldsymbol{N}$ which contains amplitude terms based on a signal-to-noise ratio:

$$\boldsymbol{S}_{\hat{p}\hat{p}} = \boldsymbol{S}_{pp} + \hat{\boldsymbol{\Gamma}} \tag{11}$$

In the context of turbocharger noise measurement, the flow generated by the compressor is at high speeds and can build up to $M_a = 0.3$ leading to heavy turbulent flows. They can be seen as local wall pressure fluctuations that can be well described with a Corcos model. The complex coherence terms Γ_{ij} are described by Corcos in [12] and can be seen as a function of i and j microphones, transversal and axial spacing Δs and Δz, the convection velocity U_c, pulsation ω and the transversal and axial coefficients γ_s and γ_z given in [13] :

$$\Gamma_{ij} = e^{-\gamma_s \omega \frac{|\Delta s|}{U_c}} e^{-\gamma_z \omega \frac{|\Delta z|}{U_c}} e^{i\omega \frac{\Delta z}{U_c}}, \hat{\Gamma}_{ij} = \Gamma_{ij} N_{ii} \tag{12}$$

The amplitude terms N_{ii} are a function of the signal-to-noise ratio SNR which is a parameter of the study. The SNR is the ratio between the auto spectrum of the acoustic pressure S_{ii} (that is without noise) and the measured auto-spectrum. A negative value of SNR corresponds to louder noise than the theoretical pressure and a positive value to a quieter noise than theoretical pressure.

$$N_{ii} = \frac{S_{ii}}{10^{\frac{SNR_{dB}}{10}}} \tag{13}$$

For the sake of illustration, the real part of the TBL coherence can be observed at two frequencies in Figure 5. This shows the pollution effect of the TBL noise between microphones concentrated at low frequencies.

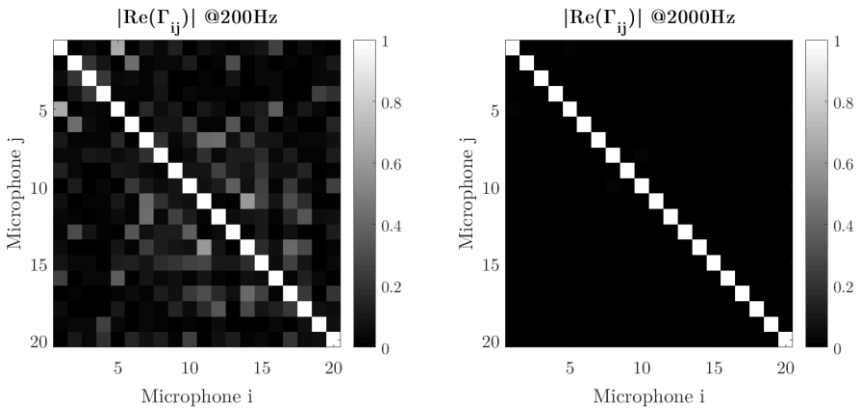

Figure 5 : Inter-microphone coherence of TBL noise (GA array)

Denoising

The TBL noise is described with a Corcos model and if the distance between two microphones is larger than the corresponding turbulence coherence length, the coherence of the noise will be close to zero. This is the hypothesis behind the Diagonal Reconstruction (DR) presented in [14]. In this case, only autospectra on the diagonal of the interspectral matrix $\boldsymbol{S}_{\hat{p}\hat{p}}$ are noised. To denoise this matrix, it is assumed that acoustic waves are all perfectly correlated which means that the new autospectra at microphones $\tilde{S}_{ii}$ should satisfy:

$$\frac{|S_{ij}|^2}{\tilde{S}_{ii}\tilde{S}_{jj}} = 1 \tag{14}$$

Using decimal logarithm as in equation (15), equation (14) can be written in a matrix form with $\boldsymbol{D}$ the vector of pressure autospectras ($D_{ii} = 10\, log_{10}\tilde{S}_{ii}$) supposed without noise, $\boldsymbol{L}$ the pressure interspectras ($L_{ij} = 20\, log_{10}|S_{ij}|$) and $\boldsymbol{U}$ the inter-microphones connectivity matrix:

$$20\, log_{10}(|S_{ij}|) = 10\, log_{10}(\tilde{S}_{ii}) + 10\, log_{10}(\tilde{S}_{jj}) \tag{15}$$

$$\boldsymbol{L} = \boldsymbol{U}\boldsymbol{D} \tag{16}$$

The Diagonal Reconstruction method gives rise to a new pressure interspectral matrix $\boldsymbol{S}_{pp,DR}$. The corresponding modal interspectral matrix $\boldsymbol{S}_{\hat{A}\hat{A},DR}$ is computed with equation (9).

Denoising performance

The denoising performance is evaluated comparing the theoretical and unnoised synthesized acoustic power and noised one using equation (7). In this parametric study three values for the modal coherence coefficient are considered (here we took respectively 0, 0.5 and 1 for all modes) as well as three values of signal to noise ratio ($SNR_{dB} = -20$, 0 and 20). Simulations are conducted on a 0.05 m diameter infinite duct and $M_a = 0.1$. In this duct, all modes travelling in both directions are excited. For the sake of clarity, negative azimuthal orders are not represented but show similar results to positive ones. In addition, in most results, positive and negative propagating modes shows very little difference so only positive ones are represented.

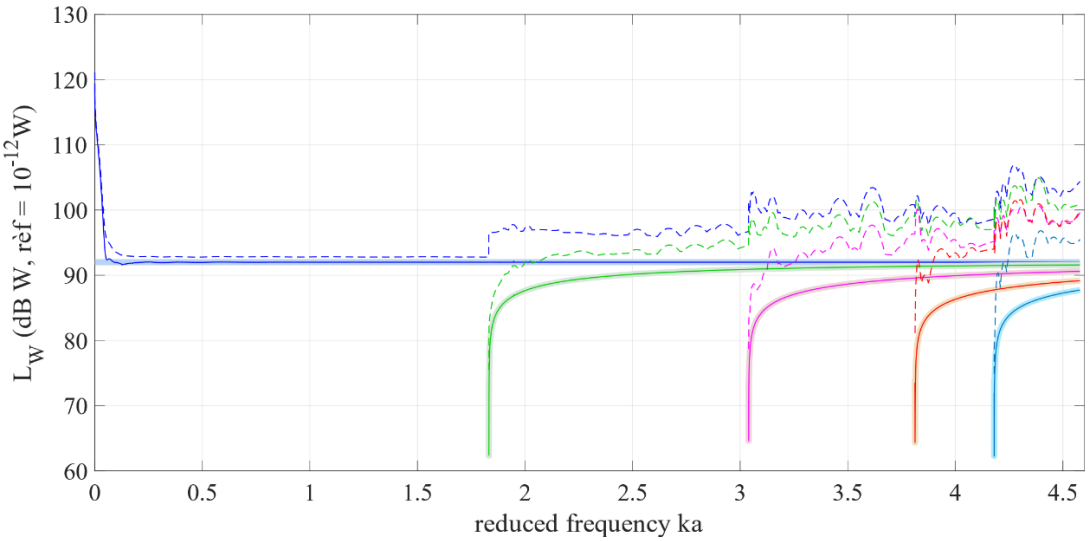

Figure 6: Denoising performance for progressive modes with $\gamma_{mn,m'n'} = 1$ and $SNR_{dB} = 0\ dB$. Blue : mode (0,0), Green : mode (1,0), Magenta : mode (2,0), Red : mode (0,1), Cyan : mode (3,0) ; Thick line : Theoretical, Dashed line : Noised, Solid line : Denoised

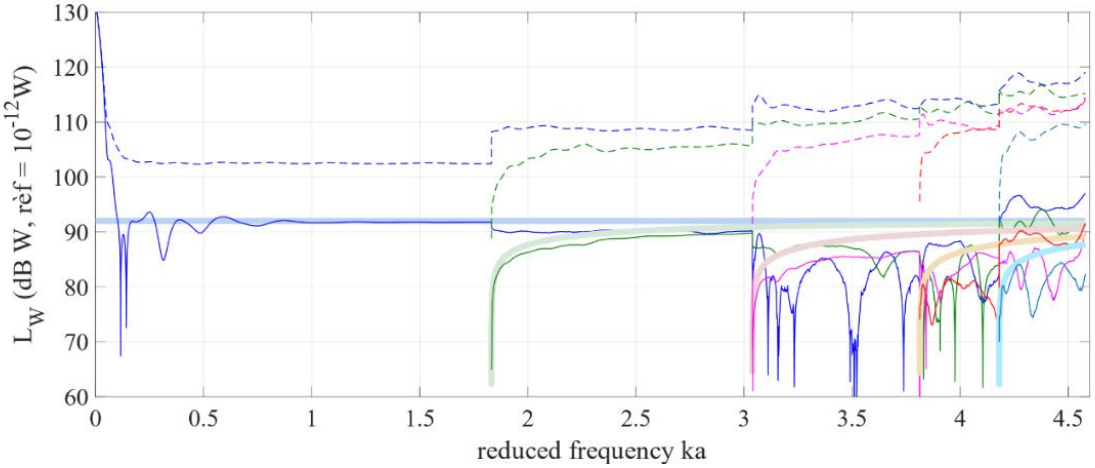

Figure 7 : Denoising performance for progressive modes with $\gamma_{mn,m'n'} = 0$ and $SNR_{dB} = -20dB$. Blue : mode (0,0), Green : mode (1,0), Magenta : mode (2,0), Red : mode (0,1), Cyan : mode (3,0) ; Thick line : Theoretical, Dashed line : Noised, Solid line : Denoised

Denoising performance represented in Figure 6 shows best results when propagating modes are all perfectly correlated with less than 1dB of difference with the theoretical acoustic power. However, a high noise level accompanied with a small modal coherence can lead to poor performances as shown in Figure 7.

A synthesis of the denoising performances is represented in Figure 8. The total acoustic power propagating in the positive direction calculated with equation (8) is shown for the 9 configurations of the parametric study. For 0 dB and 20 dB all curves are covered for any modal coherence, this shows that the Diagonal Reconstruction works well for low to moderate TBL noise levels relatively to the analyzed pressure. With the information of Figure 5, it can be observed that results below 1 kHz are mainly driven by the correlation length of the turbulent flow whereas at higher frequency (say one above 1 kHz) the quality of reconstruction is driven by the modal coherence. When duct acoustic modes are perfectly correlated, the DR method is efficient. When modal coherence is below 1, the technique can still deliver reasonable results. When modes are totally uncorrelated, one can observe a very strong deviation especially above the cut-off frequency of the first radial mode and in this scenario the DR method should be avoided.

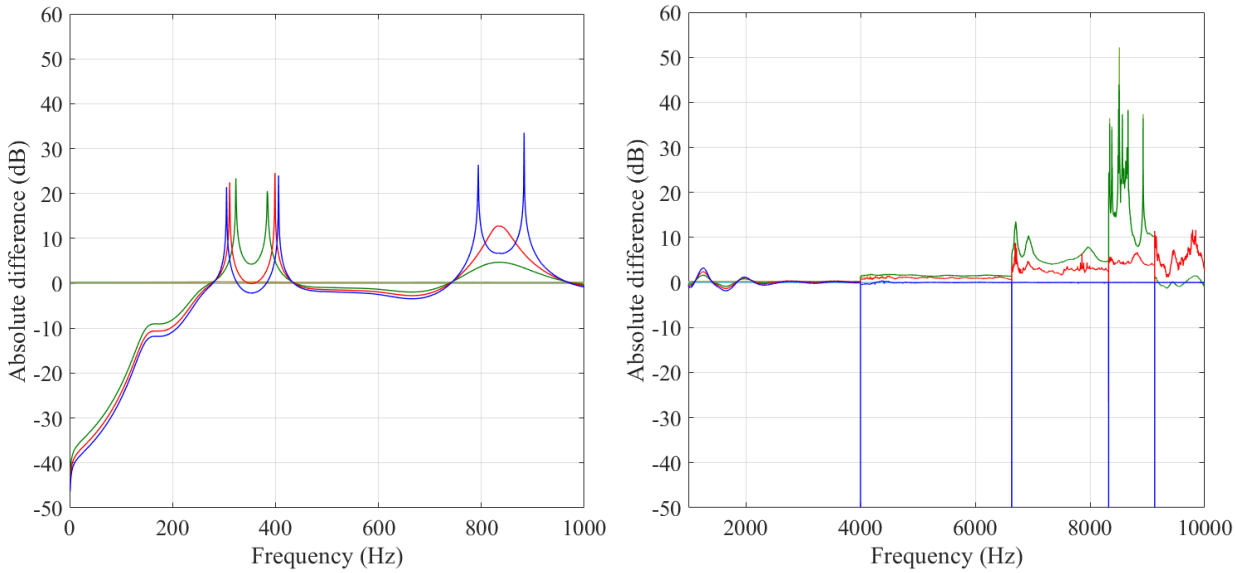

Figure 8 : Absolute difference between theoretical and denoised total acoustic power :
Blue : $\gamma = 1$, *Red :* $\gamma = 0{,}5$, *Green :* $\gamma = 0$
Dark colour : $SNR_{dB} = -20\ dB$, *normal colour :* $SNR_{dB} = 0\ dB$, *light colour :* $SNR_{dB} = 20\ dB$

CONCLUSION

In this paper a comparison of several techniques for microphones positioning are presented. The use of a genetic algorithm allowed to obtain a nearly optimal microphone array in a circular duct that minimizes the condition number of the collocation matrix which relates the pressure at the microphones to the modal amplitudes of the duct acoustic modes. The performances of the denoising technique have been shown. It is demonstrated that the Diagonal Reconstruction is very reliable as long as modal coherence is sufficiently high (say above 0.5) and turbulent boundary layer noise not higher than the measured acoustic pressure without noise. Work is ongoing by the authors to develop a full 2N-port model for the turbocharger characterization.

ACKNOWLEDGMENTS

The authors would like to acknowledge the financial support from the ANRT and CRITT M2A grant.

BIBLIOGRAPHY

[1] *Evolution du parc et des immatriculations entre essence et diesel* http://www.fiches-auto.fr/articles-auto/l-auto-en-chiffres/s-891-immatriculations-essence-diesel.php (accessed Dec. 06, **2021**)

[2] R. Kabral and M. Åbom - *Investigation of turbocharger compressor surge inception by means of an acoustic two-port model*, Journal of Sound and Vibration, vol. 412, **2018**

[3] S. Sack, M. Åbom, and Efraimsson - *On Acoustic Multi-Port Characterisation Including Higher Order Modes*, Acta Acustica united with Acustica, vol. 102, no. 5, **2016**

[4] S. Sack, M. Åbom, C. F. Schram, and K. Kucukcoskun - *Generation and scattering of acoustic modes in ducts with flow*, Proceedings of 20th AIAA/CEAS Aeroacoustics Conference, Atlanta, GA, **2014**

[5] S. Sack and M. Åbom - *Trained Algorithms for Mode Decomposition in Ducts*, in 23rd International Congress on Acoustics, Aachen, **2019**

[6] I. Jaimes, A. Millot, and J. Charley - *Acoustic characterization of the compressor stage of an automotive turbocharger*, in 23ème Congrès Français de Mécanique, Lille, **2017**

[7] S. Bennouna, S. Naji, O. Cheriaux, S. Moreau, B. Ouedraogo, and J. M. Ville - *Aeroacoustic Prediction Methods of Automotive HVAC Noise*, Proceedings of SAE 2015 Noise and Vibration Conference and Exhibition, Grand Rapids, Michigan, **2015**

[8] H. Trabelsi, N. Zerbib, J.-M. Ville, and F. Foucart - *Méthode de mesure de la matrice de diffusion multimodale d'obstacles complexes en présence d'écoulement uniforme*, in 10ème Congrès Français d'Acoustique, Lyon, **2010**

[9] C. L. Morfey - *Sound transmission and generation in ducts with flow*, Journal of Sound and Vibration, vol. 14, no. 1, **1971**

[10] M. Åbom and H. Bodén - *Error analysis of two-microphone measurements in ducts with flow*, The Journal of the Acoustical Society of America, vol. 83, no. 6, **1988**

[11] U. Tapken and L. Enghardt - *Optimisation of Sensor Arrays for Radial Mode Analysis in Flow Ducts*, Proceedings of 12th AIAA/CEAS Aeroacoustics Conference (27th AIAA Aeroacoustics Conference), Cambridge, Massachusetts, **2006**

[12] G. M. Corcos - *Resolution of Pressure in Turbulence*, The Journal of the Acoustical Society of America, vol. 35, no. 2, **1963**

[13] A. David, F. Hugues, N. Dauchez, and E. Perrey-Debain - *Vibrational response of a rectangular duct of finite length excited by a turbulent internal flow*, Journal of Sound and Vibration, vol. 422, **2018**

[14] A. Finez, A. Pereira, and Q. Leclere - *Broadband mode decomposition of ducted fan noise using cross-spectral matrix denoising*, in 2015 International Conference on Fan Noise, Aerodynamics, Applications & Systems, Darmstadt, **2015**